

# Detection and documentation of a submerged neolithic pile dwelling settlement using airborne laser bathymetry and multimedia photogrammetry - A case study at lake Mondsee

Katharina Riederer, David Simböck, Gottfried Mandlbürger

<sup>1</sup>Department of Geodesy and Geoinformation, TU Wien; 1040 Vienna, Austria  
[katharina.riederer, david.simboeck, gottfried.mandlbürger]@geo.tuwien.ac.at

**Keywords:** airborne laser bathymetry, multimedia photogrammetry, archaeology, pile dwellings, cultural heritage, lake dwelling

## Abstract

This study presents a comparative analysis of airborne laser bathymetry (ALB) and multimedia photogrammetry for the detection and documentation of a submerged Neolithic pile dwelling settlement in Lake Mondsee, Austria. High-resolution ALB data acquired with a UAV-mounted bathymetric laser scanner and aerial images were processed and evaluated for suitability to identify submerged wooden piles and associated archaeological features. The results demonstrate that ALB delivers superior data quality, allowing the detection of small-scale structures even at depths of up to 7 m, while multimedia photogrammetry was limited by water turbidity and depth, with reliable results only up to 3 m. Despite its limitations, photogrammetry proved useful for larger features under favorable conditions. The study confirms ALB as the more robust technique for detailed underwater archaeological documentation in moderately turbid lake environments.

## 1. Introduction

### 1.1 Motivation

The pile dwelling settlement of See am Mondsee, classified by UNESCO as a World Heritage Site, is a Neolithic (3800-3400 BC) settlement in a shallow lake area. The remains of this settlement are piles of up to 45 cm height, although not all of those piles have yet been precisely detected (Pohl, 2016). As noted in (Doneus et al., 2015; McCarthy, 2014), both airborne laser bathymetry (ALB) and multimedia photogrammetry can be effective and efficient methods for continuous documentation and the subsequent preservation of cultural heritage. However, data processing is challenging, especially in lakes, due to the turbidity of the water (Doneus et al., 2015).

In addition to natural decay and human intervention, the permanent monitoring of the pile dwelling settlement since 2013 has made it possible to determine that global warming is also leading to increasingly poorer conservation conditions. Increasingly severe storms and the resulting anchor drag also pose an immense risk to the World Heritage Site (Pohl, 2016; McCarthy, 2014).

Taking the above into account, this poses the question as to what extent the resolution and quality of ALB and multimedia photogrammetry measurements allow for the detection of those submerged structures. In addition, the question arises whether one of the two methods is better suited to this task or whether one of them has clear advantages over the other in this respect.

### 1.2 Data acquisition

In March 2022, Skyability GmbH carried out a drone flight over Lake Mondsee, seen in Figure 1, in Upper Austria to record the settlement of pile dwellings located there using both ALB and multimedia photogrammetry. The survey area is located in the eastern part of Lake Mondsee (47.803889 N, 13.449167 E) and extends approximately 230 m x 135 m. The laser survey was

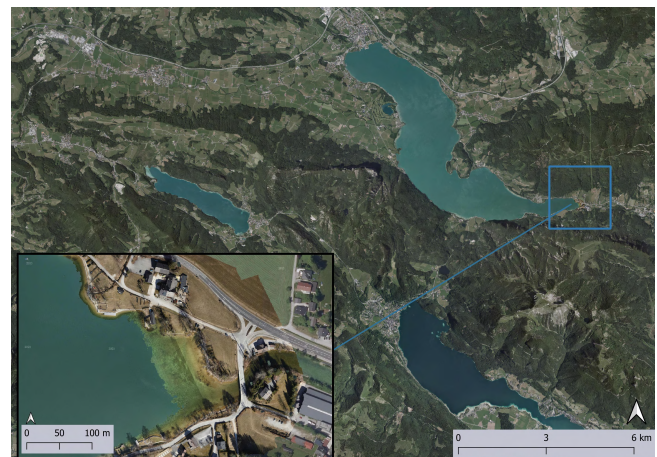


Figure 1. Overview of lake Mondsee and location of the archaeological site.

carried out with the topo-bathymetric laser scanner *RIEGL VQ-840-G* and the photographic survey with a *DJI Zenmuse P1 40 Mpix RGB* camera. In both cases, the sensors were carried by a multi-copter UAV. The laser scanner used was operated with a pulse repetition rate of 50 – 200 kHz and a laser footprint of 15 cm.

### 1.3 Archaeological site

The remains of the pile-dwelling settlement of See am Mondsee lie at a depth of around 1.8 m to 5 m on a beach plate (Pohl, 2023). After the pile-dwelling settlements around the Alps were classified as a UNESCO World Heritage Site in 2011, regular research work and preventive measures for protection have been carried out since 2013 (Pohl, 2016). First, erosion markers were systematically placed within the settlement remains in 2013 to observe and measure permanent change in the context of erosion (Dworsky et al., 2025). By 2014, the settlement's

hazard zones could already be identified and summarized by (Pohl, 2015):

- Cultivated layer only 2 cm to 6 cm covered by protective layer - it moves during storms and tempests.
- The erosion markers have eroded 1 cm to 3 cm in 1.5 years - still within tolerance, provided that the trend does not increase.
- Several erosion markers were placed directly before a strong storm and, therefore, could be checked immediately afterward. Observations show that even a weak westerly wind (main wind direction) is sufficient to trigger high waves in the area of settlement structures. As a result, the artifacts and cultural layer are moved and damage can occur.
- Strong currents remove sediment from the lake bed, which leads to erosion. Increasingly severe weather events due to man-made climate change are expected to cause more damage.

Between 2013 and 2021, erosion was observed in a range of 1 cm to 8 cm (Pohl, 2021). In 2018, erosion damage, especially to the edges of the profile, of the old excavation section (in Figure 2; labeled A) by Johannes Offenberger of 1982 could be detected during an underwater inspection (Pohl, 2018). For this reason, the entire old excavation section (A) was covered with a geotextile, made mainly of bast fabric, during another campaign in 2020, to prevent further damage (Pohl, 2020). According to (Pohl, 2015), the occurrence of storms and wind cannot be the decisive reason for the increase in erosion and damage that has occurred in recent years. There must be other factors, as yet unknown, that are accelerating the erosion process. Archaeology cannot answer this question without the participation of other disciplines. Bathymetry and current measurements should therefore provide a remedy here (Pohl, 2015). In addition, (Dworsky et al., 2025) states that the Federal Office of Water Management can determine an average surface water warming of 2° C between 1975 and 2015. During the work between 2013 and 2021, a considerable increase in macrophytes can be observed, which, on the one hand, support conservation, but, on the other hand, destroy and affect the anthropogenic culture layer through root formation (Pohl, 2015).

## 2. Method and Data processing

### 2.1 Airborne Laser Bathymetry

Airborne laser bathymetry (ALB) is an active remote sensing method, in which green laser light with a wavelength of  $\lambda \approx 532\text{nm}$  is used to record the topography of water bodies. For this purpose, a multisensor system consisting of a laser scanner, a GNSS receiver, and an IMU is mounted on a flying object like a drone or airplane (Mandlbürger, 2020). During a measurement flight, the laser scanner emits a series of short laser pulses which travel through the air, to be reflected, transmitted, or absorbed either in parts or as a whole from different surfaces and media they encounter. The reflected portion of those pulses is received by the ALB-sensor. The time difference between the emission of a signal and the detection of its echos is used to calculate the distance between the sensor and the measured point. Additionally, the deflection angles of every

sent laser pulse are recorded inside the scanner (Pfeifer et al., 2017). Combining the data acquired by the laser scanner with the positional and rotational data from GNSS and IMU allows the calculation of global coordinates for the measured points (Kraus, 2004). The resulting point cloud contains not only geometrical but also radiometric information such as amplitude, reflectance, or echo width (Pfeifer et al., 2017).

In the case of ALB the sent-out light has to travel through two different media with varying optical properties. As the propagation speed of light in water is lower than in air, the laser pulse is redirected at the water surface. This effect is known as refraction and is mathematically described by Snell's law. It leads to a systematic underestimation of the ground height within water bodies and therefore must be corrected for in data processing (Mandlbürger, 2020). As the refraction angle depends on the incident angle, this angle remains relatively constant at  $\pm 1^\circ$  over the scan range of up to  $60^\circ$ , resulting in an elliptical or circular scan pattern (Mandlbürger et al., 2011). A more detailed description of the concept and most important mathematical relations of ALB and laser scanning, in general, is given in (Pfeifer et al., 2017; Philpot et al., 2019).

**2.1.1 Data processing:** Data processing was performed according to (Mandlbürger et al., 2015; Doneus et al., 2015), mainly using the ALS processing software OPALS (Mandlbürger et al., 2009). Due to the smooth state of the water surface during the measurements, a simplified water surface model (WSM) was used for subsequent refraction correction (Mulsow et al., 2020). Although echo detection was conducted through online waveform processing from the RIEGL VQ-840-G directly (RIEGL, 2025), RiProcess software was used to generate a georeferenced 3D point cloud for each flight strip. The complete data set consists of 9 flight strips and their respective trajectory files. The fifth percentile of the point density - only considering the last echos - in each individual strip is at least  $80\text{ pts}/\text{m}^2$ . The combined point cloud contains about 112 million points and shows a point density with a fifth percentile of at least  $150\text{ pts}/\text{m}^2$ .

To derive a simple WSM, water surface points were classified by thresholding the amplitude and height of all echos. From those points a WSM was generated, using a moving planes interpolation to rasterize the point data. In combination with the trajectory, recorded by the GNSS and the IMU, a refraction correction was performed, as described in (Mandlbürger et al., 2013; Philpot et al., 2019).

Subsequently, a robust hierarchic interpolation as discussed in (Pfeifer and Mandlbürger, 2018) was applied to the point cloud to extract the terrain points. The interpolation was performed in 5 Pyramid levels using filter thresholds of 0.2 m, 0.5 m, 1.0 m, 2.5 m and 4.0 m. Following the classification of the terrain points, a digital terrain model (DTM) was generated using moving planes interpolation. Due to the relatively high point density, a spatial resolution of 0.025 m could be achieved. Finally, a water depth map was calculated by subtracting the DTM from the WSM. The aforementioned steps were performed, using the scientific laser scanning software OPALS (Mandlbürger et al., 2009; Pfeifer et al., 2014).

**2.1.2 Visualization and Interpretation:** To enable a visual interpretation of the data, a hill-shade and a height-coded map were derived from the DTM using OPALS. Archaeological interpretation as described, e.g. in (Doneus et al., 2013; Opitz and Cowley, 2013) was carried out using the open source

GIS-Environment QGIS. The goal of this interpretation was to identify as many piles as possible within a predefined area. This would then be followed by an evaluation of the certainty of those identifications. During the interpretation process two main difficulties arose, which will be discussed in more detail.

- Several piles are relatively small and, in some areas, densely accumulated, making them harder to identify than larger structures, for example, the ones investigated in (Doneus et al., 2013, 2015).
- An adequate evaluation of the extent to which the interpretation of these data is suitable for the detection of the piles requires a comparison with reference data. Unfortunately, such reference data, with sufficient accuracy, were hard to come by in this case.

Although there is no substitute for having independent reference data, another approach shall be explored in the following. A possible way, if not to validate, then at least to strengthen the interpretation, could be an alternative visualization that allows for a better identification of different structures. Piles and other submerged objects like stones can have similar extents, making them hard to differentiate when viewed from above. Bigger differences can be expected in the height and slope of the piles compared to those of the other structures. Through interpolation conducted during the derivation of the DTM, the geometry of the piles is flattened and smoothed, resulting in further loss of distinctive features (Kraus, 2004). Therefore, piles should be better detectable in the profile of the refraction corrected point cloud. The disadvantage here is the reduction of the geometrical information to only two dimensions. Combining the classical interpretation of the DTM, to gain an overview of the whole area of interest, with an interpretation of a point cloud profile, could yield great results. In relevant areas, the profile could be used to give a detailed view of the scene, which can help to validate the DTM interpretation. To test if this holds true, two profiles from the refraction-corrected point cloud were visualized. The placement and orientation was chosen so that multiple potential piles were intersected in uncertain areas.

## 2.2 Multimedia photogrammetry

Multimedia photogrammetry is a passive photogrammetric measurement method (Jutzi et al., 2017). Unlike acoustic methods, such as SONAR (Sound Navigation And Ranging), it usually records data on land and in the air (Gueguen and Mandlbürger, 2024). The aim of this method is to reconstruct the underwater topography. As light reflected from the water surface is photographed, the transition from the optically thinner medium of air to the optically denser medium of water must be considered. In this context, we refer to this as multimedia photogrammetry (Maas, 2014). The refraction caused by this change of medium can be corrected using Snell's law of refraction. This enables light rays to be reconstructed in a refraction-corrected manner, contributing to a more precise depth determination (Mandlbürger, 2019a).

Two different data sets were recorded on the same day. One was captured from a flying altitude of 90 m above ground level (agl), containing a total of 390 images. The other was captured at a height of 120 m and contains 375 images. The entire aerial survey of the photogrammetric images took ten minutes at each flight altitude. Although the exact weather conditions on this day cannot be reconstructed, the photos show that it was cloudy

throughout and the water appeared quite turbid. The drone's internal GNSS is used for georeferencing. In the water area, images were acquired with a longitudinal overlap of 94.5% and a transverse overlap of 65%. The entire area recorded with the drone covers 430 m x 300 m, with the water area measuring only 120 m x 80 m.

The multimedia photogrammetric data was processed and tested with different software. The following were used: (i) Agisoft Metashape ([www.agisoft.com](http://www.agisoft.com)), (ii) Pix4D Mapper ([www.pix4d.com](http://www.pix4d.com)), (iii) nFrames SURE ([www.nframes.com](http://www.nframes.com))

In the following, the workflows in the three software packages are compared and evaluated. The general workflow of all three software packages follows (Gueguen and Mandlbürger, 2024; Mandlbürger et al., 2025), starting with (i) aligning the photos, i.e. calculating the outer orientation of the cameras (X, Y and Z coordinates of the projection center and the three rotation angles roll, pitch, and yaw) using a bundle-block adjustment (Mulsow, 2010). (ii) Camera calibration is improved and (iii) dense point cloud is calculated (Mandlbürger et al., 2025). As no control points (GCPs) were recorded during the data collection process, they cannot contribute to improving the accuracy of the model. According to (Mandlbürger, 2019b), the orientation of the images through bundle block adjustment, the calculation of the inner and outer camera orientations, and the determination of the image distortion are essential to achieve a high-resolution surface reconstruction.

**2.2.1 Agisoft Metashape:** Agisoft Metashape is a comprehensive software solution for all photogrammetric processes. The following results were generated using only the user interface and standard parameters. The aim is to process the data as efficiently as possible so that archaeologists will have faster access in future.

For this application, flight data from an altitude of 120 m is used and exported at high resolution as a point cloud to perform a refraction correction and calculate a digital terrain model (DTM). Additionally, the external orientations of the cameras are exported from this project (reason can be seen below). With bundle block adjustment in Agisoft Metashape, 368 of a total of 375 photos can be oriented, with the missing 7 photos showing only the water surface.

**2.2.2 SURE:** For dense image allocation in the SURE application, an adapted Python script by Mandlbürger (2021) is used to orient the images in pairs in the following pattern: [Img 1, Img 3], [Img 2, Img 4], [Img 5, Img 7], etc. This is because the images overlap by more than 90%, so a larger distance between the stereo images could provide better results, especially in the water. The image pairs are oriented towards each other by detecting corresponding tie points in both images, which are then used directly to create a point cloud. This was tested at altitudes of both 90 and 120 m. However, 90 m altitude proved impractical as the low altitude meant that fewer tie points could be found, so no alignment was possible for most of the image pairs. It is also worth mentioning that the external orientation of the cameras, which was previously calculated in Agisoft Metashape, was used to align the photos.

**2.2.3 Pix4D:** In Pix4D, images can be imported directly with known external camera orientations. The software offers the option to calculate these orientations itself or to use previously computed values, for example, from Agisoft Metashape.

In this study, the former approach was chosen to allow independent testing of Pix4D software. A major advantage of Pix4D is its comprehensive quality report, which documents the entire processing workflow—from image acquisition to point cloud generation. The report provides useful statistical parameters and accuracy metrics that allow a detailed evaluation of the results.

**2.2.4 Study areas:** Due to the large amount of data, two small study areas were selected for analysis. Both study areas are extracted from the three point clouds generated with the different software. The extent was cropped out using the point cloud processing software OPALS. The first study area is a narrow 60 m x 5 m strip with a north-south orientation from the shore into the lake and can be seen in Figure 5. The second study area is a 40 m x 25 m rectangle containing the measurement grid (D) mentioned above in Figure 6 on the right side. Flight data from a height of 120 m is used for the evaluation. After narrowing down and thus reducing the amount of data, the study areas are corrected for refraction following the approach mentioned in Section 2.1.1. As already mentioned in (Mulsov et al., 2020), it is difficult to reconstruct the water surface from the bundle block adjustment if only nadir images are available. For this reason, the water surface is assumed horizontal with a constant height of 526.45 m. The results of the different outcomes are discussed below.

### 3. Results

#### 3.1 Laserbathymetry

**3.1.1 DTM interpretation:** The shading of the digital terrain model in Figure 6 on the left side clearly shows various submerged structures in remarkable detail. Due to the high spatial resolution of 2.5 cm the interpretation allowed the detection of single piles, as well as wooden planks and logs. The results of a GIS-based archaeological interpretation (Opitz and Cowley, 2013) can be seen in Figure 2, although only exemplary parts of the pile field were analyzed. The outline of the cultural layer could not be detected in the DTM and is therefore estimated on the basis of archaeological excavation data. The extent of the actual pile field, on the other hand, can be derived as an outline around the area where piles are identified within the DTM. The result mostly corresponds to the extent suggested from archaeological data. Structure (A) was identified as a trench from an archaeological excavation done by Offenberger in the 1980s. The erosion protection mats installed in 2020 and 2021 could not be detected in the DTM, but their estimated extent and location according to (Pohl, 2021) are indicated by (B) and (C). The big measurement grid (D) used in another excavation conducted by Offenberger in the 1980s is clearly visible, though the deepest lying section of the grid is rather faint. All the aforementioned archaeological reference data can be found in (Pohl, 2021; Pohl et al., 2023).

Although larger-scale structures could be detected fairly easily, the identification of potential piles is more difficult. Like mentioned in 2.1.2, the different extents of the piles, possibly corresponding to the size of other submerged objects, lead to great ambiguity in interpretation. The dense clustering of piles in some areas, such as around the excavation grid (D), further increases the uncertainty. According to (Pohl, 2016), the piles have a height up to 0.45 m. All structures that appeared reasonably steep and were of suitable size were considered potential piles. In Figure 2 they are marked in brown, whereas other



Figure 2. GIS-based interpretation of the pile-dwelling settlement See/Mondsee based on the digital terrain model derived from the laserbathymetric data.

wooden objects supposed to be planks and logs are marked in beige. The interpretation may be ambiguous, but the aim of this paper was to determine whether the resolution and quality of optical bathymetric methods allow for the detection of submerged piles. As for ALB, it can be said that these requirements are fully met, due to the detailed depiction of the lake floor showing structures even smaller than the smallest archaeologically verified piles (Dworsky et al., 2025).

**3.1.2 Point cloud interpretation:** With the goal of increasing the certainty of the DTM interpretation multiple exemplary profiles along rows and through clusters of supposed piles were cut out of the refraction corrected point cloud. In Figure 4 these profiles (profile A and B) are shown together with the respective interpretation of the DTM. The interpreted structures were labeled with the roman numerals 1 to 14 and are henceforth referred to accordingly. To increase the contrast of the submerged structures with the surrounding lake bed, the point cloud was colored according to the reflectivity obtained from the radiometric information of the respective echos. In Figure 3 an accordingly colored subset of the point cloud shown in bird's-eye view, depicts the high contrast in reflectance between submerged objects and the lake bed. However, a differentiation of piles and other objects such as stones based on reflectance alone could not be made.

The interpretation shown in Figure 4 yielded results, which are discussed below. In profile A, at least 11 different objects could be detected, though structure (III) most likely consists of multiple objects. In this case, the DTM interpretation provided clarification, as at least two separate objects can be seen from this perspective. In all other cases, the comparison with the point cloud seemed to generally help verify, or in some cases disprove, the interpretations of the DTM. Structures (I), (IV), (V), (VII), (VIII), and (X) show realistic heights and proportions over all, to be interpreted as piles. For all of them, the corresponding objects with appropriate coordinates can be found in the DTM. Although (VI) and (XI) appear to be high enough to be considered piles, the lack of measured points and their vague appearance in the DTM make the interpretation uncertain. In contrast, (II) and (IX) can clearly be seen in the DTM but should instead be considered stones because of their heights and diameters.

Profile B shows five distinct objects and intersects profile A.

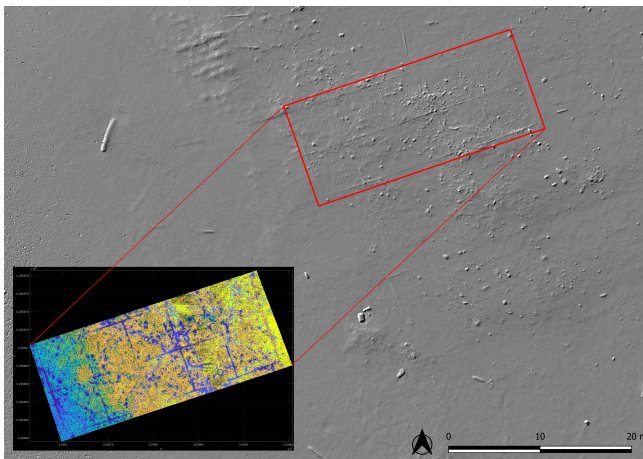


Figure 3. Area around the measurement grid (A) shown in the DTM and the point cloud (bottom left corner); the latter is color-coded according to its reflectance

Therefore, both structures (VIII) and (IX) can be seen from two different perspectives, helping to interpret the situation. Although structure (XII) appears like one flat object, the corresponding area in the DTM allows for the differentiation of at least three objects, most likely stones. Finally, (XIII) and (XIV) also appear to be stones, considering their geometry and height.

### 3.2 Multimedia Photogrammetry

As the water area is still relatively large and many drone photos show mostly water, it is difficult to achieve dense image matching in large parts (Mandlbürger, 2019b). Especially at an altitude of 90 m, the pairwise image matching with the SURE software did not work well. For some image pairs, no tie points could be identified, which meant that no point cloud could be created. Of the total of 195 pairs, only 23 pairs could be correctly orientated and a resulting point cloud was generated. The image pairs that could not be oriented were images that contained only water. For such scenarios, a special approach is needed for multimedia bundle block adjustment (Mulso, 2010). The result was significantly better for photos taken at an altitude of 120 m, with only 12.5 percent of the 87 image pairs unable to be matched. Here, too, it was found that the water-only photos were the cause. This is probably due to the flight altitude, as it becomes more likely that land points are also visible on the photos, which facilitates and improves the bundle block adjustment (Mandlbürger, 2019a). The ground sampling distance of the 90 m data is 1.15 m and for the 120 m data 1.53 cm, i.e., slightly lower resolution. The 120 m flight data is also used for the other tested software to enable a direct comparison.

Few, only very large objects are recognizable on the three models. The tree trunk seen in Figure 5 is clearly visible on the terrain model of Pix4D (middle) and Metashape (top). However, on the DTM of the tested software SURE (bottom), it is not. Since the image pairs were controlled with a Python script for evaluation purposes, a larger distance between the stereo pairs could possibly improve the result, especially in view of the fact that the overlap area was very large (sometimes 90% lengthwise).

Figure 5 shows the standard deviations of the surface normals ( $\sigma_0$ ) with a corresponding color coding for any of the three tested software. However, it is visually perceptible in the three

models in Figure 5 that  $\sigma_0$  in the deepest lake areas (west in the image) appears significantly higher than in the shallow water areas. This is particularly visible in the Agisoft Metashape product (Figure 5, top). In addition, the  $\sigma_0$  values in the Pix4D model (middle) are significantly higher, namely between -2.0 and +2.5, while the other two results are only in the range between -0.05 and 0.05. In order to improve the general data quality, it could be considered to take additional oblique images with the drone. This has the advantage of a larger recording angle, which in turn improves the cutting geometry of the model. For more precise measurement results, ground control points could be placed under water in future surveys; this is particularly useful if regular surveys are carried out using both laser and photobathymetry. (Mulso et al., 2020).

## 4. Conclusion

The visual interpretation of the models derived from the data acquired through ALB and multimedia photogrammetry shows the capabilities of both methods with respect to detection and, therefore, documentation of submerged archaeological sites. When comparing the results of both methods shown in Figure 6, it becomes clear that ALB is the superior method for the given task. Although ALB yields usable results at depths of up to 7 m, the photo bathymetric data are limited to a maximum of 3 m, which can be seen in Figure 7. As discussed in 3.2, the noise of the data acquired from multimedia photogrammetry intensifies with increasing depth of the water. Given the already generally high noise of this data set it becomes apparent that the quality of the data does not support an archaeological interpretation of the relatively small piles. However, larger structures such as the measurement grid (D), shown in Figure 6, can be seen in the data. Therefore, this evaluation of the usability of photo bathymetric measurements for the detection of submerged archaeological sites cannot be generalized. Rather, this assessment refers to the quite specific use-case of detecting small structures like the piles in this survey. It should also be noted that additional limiting factors, such as the aforementioned lack of ground control points (GCPs) and the less than optimal water conditions (turbidity of the water) during flight, made it considerably more difficult to analyze the data. Whether there might be a more suitable time of year to take the photos remains to be clarified in the future. In conclusion, multimedia photogrammetry might yield better results for this task depending on the circumstances of the survey. For ALB, on the other hand, the quality of the data enables the detection of various small-scale structures. Although differentiating between them proves difficult using only the DTM, an additional interpretation of point clouds as shown in Figure 4 simplifies the detection and distinction of piles and other submerged objects.

As already mentioned in Section 1.3, macrophytes have a positive effect on pile preservation conditions. However, this comes with a downside: Their roots interfere with the anthropogenic layers and thus can cause destruction in the archaeological site (Pohl, 2015). In this context, the detection of macrophytes using ALB could supplement the monitoring of submerged piles and their preservation conditions. An approach like the one described in (Rhomberg-Kauert et al., 2024), could be well suited to the task.

Finally, the increasing use of deep learning models, especially NeRF algorithms, in recent years could significantly improve photobathymetry. Therefore, they could potentially also play a

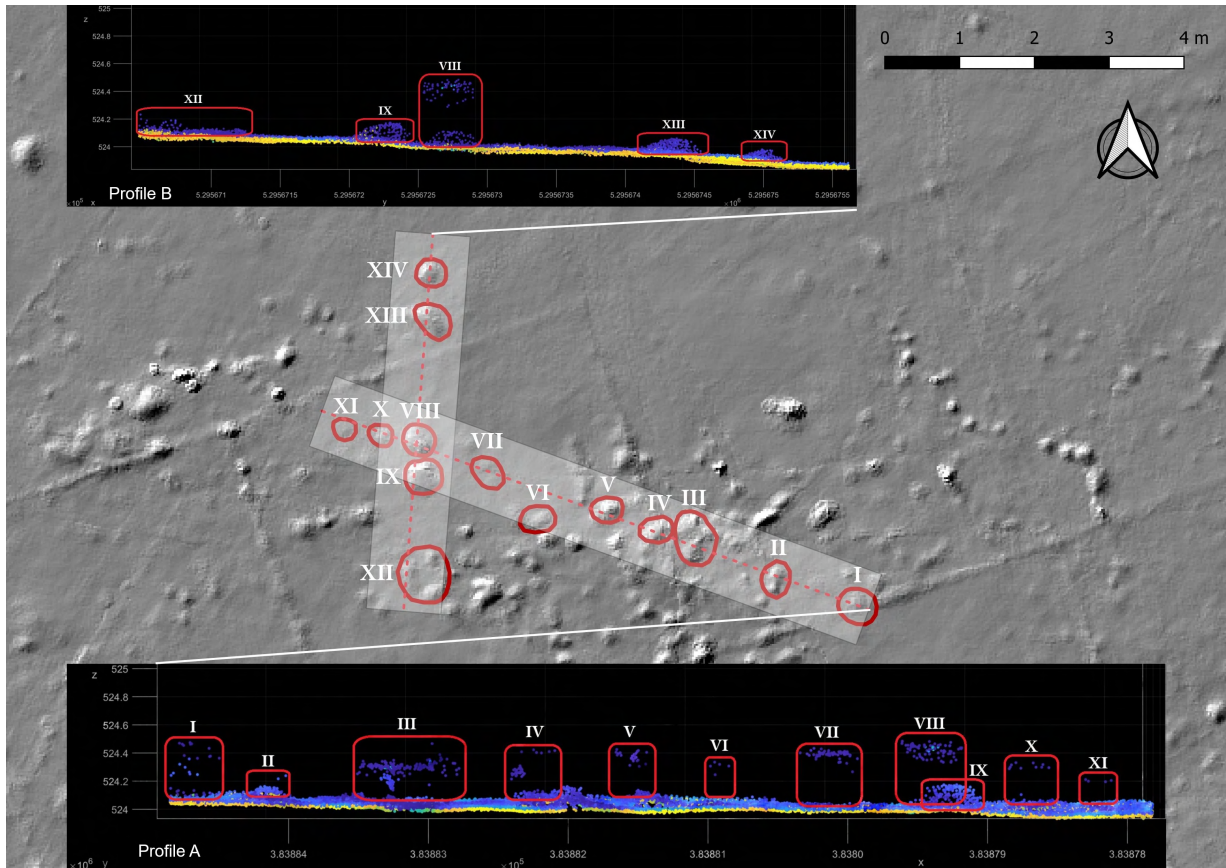


Figure 4. Interpretation of DTM (hillshade) and point cloud profiles (bottom: A, top: B); profiles marked with red dotted lines

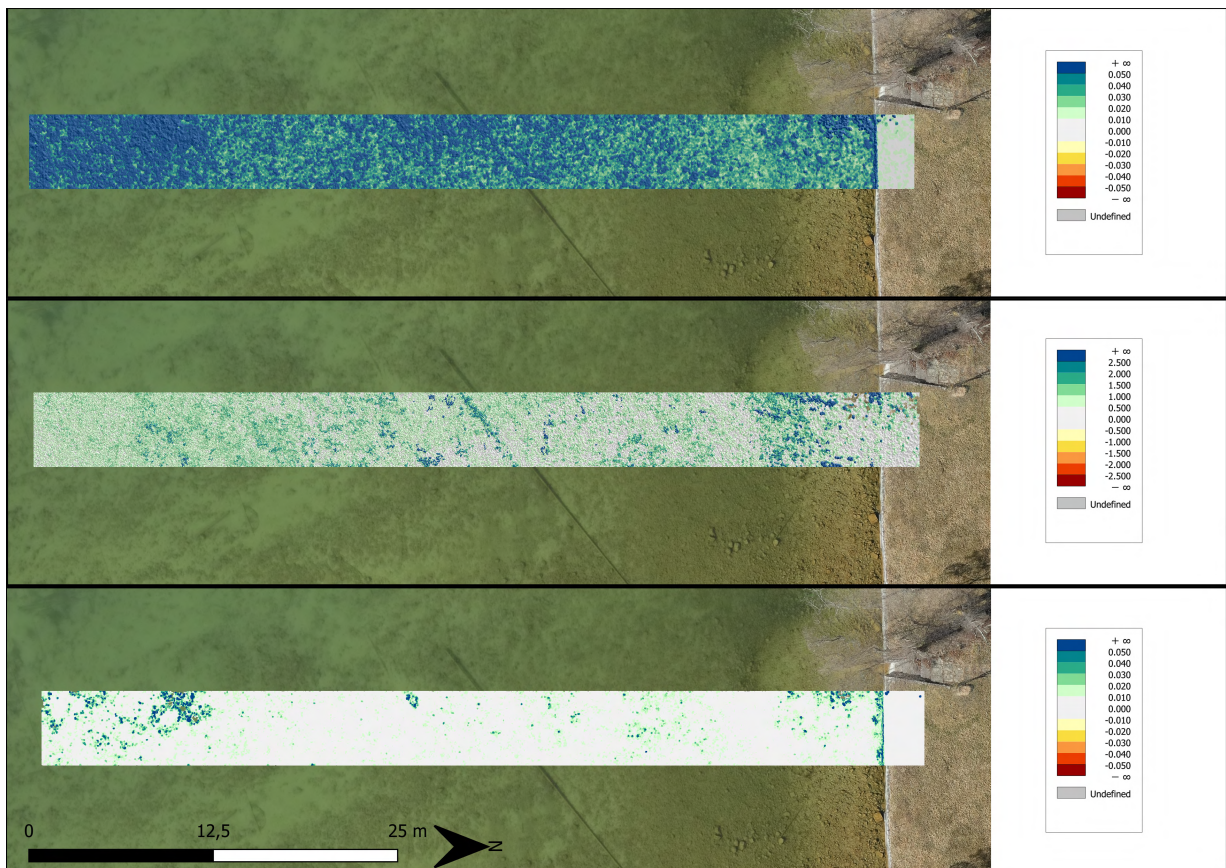


Figure 5. Study area 1, color-coded representation of sigma0. Top: Agisoft Metashape; Middle: Pix4D and Bottom: SURE.

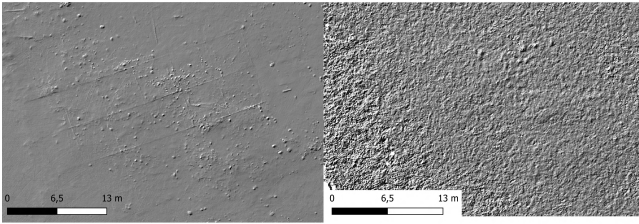


Figure 6. Results of the DTMs created. Left: DTM from the refraction-corrected ALB data and right: DTM from the refraction-corrected photobathymetry data (Pix4D).

relevant role in the documentation of archaeological underwater sites (Mandlbürger et al., 2025; Mildenhall et al., 2020).

### Acknowledgements

Many thanks to the team of Skyability GmbH and David Monetti especially for providing the data. Also, thanks to Cyril Dworsky for scientific support on the archaeological side.

### References

Doneus, M., Doneus, N., Briese, C., Pregeßbauer, M., Mandlbürger, G., Verhoeven, G., 2013. Airborne Laser Bathymetry: Detecting and Recording Submerged Archaeological Sites from the Air. *Journal of Archaeological Science*, 40(4), 2136–2151.

Doneus, M., Miholjek, I., Mandlbürger, G., Doneus, N., Verhoeven, G., Briese, C., Pregeßbauer, M., 2015. Airborne laser bathymetry for documentation of submerged archaeological sites in shallow water. *International Archives of the Photogrammetry, Remote Sensing and Spatial Information Sciences, Volume XL-5/W5, Underwater 3D Recording and Modeling, 16–17 April 2015, Piano di Sorrento, Italy*, International Society for Photogrammetry and Remote Sensing (ISPRS), Piano di Sorrento, Italy, 99–107. Peer-reviewed contribution, Commission V.

Dworsky, C., Pohl, H., Seidl da Fonseca, H., 2025. Monitoring von unterwasserdenkmälern in Österreich am beispiel des unesco-weltkulturerbes ”prähistorische pfahlbauten um die alpen.”. *Österreichische Zeitschrift für Kunst und Denkmalpflege*, Österreichisches Bundesdenkmalamt.

Gueguen, L.-A., Mandlbürger, G., 2024. Lab experiment for photo bathymetry. Simultaneous reconstruction of water surface and bottom with a synchronised camera rig. *Hydrographische Nachrichten*.

Jutzi, B., Meyer, F. J., Hinz, S., 2017. Aktive fernerkundungs-sensorik - technologische grundlagen und abbildungsgeometrie. C. Heipke (ed.), *Photogrammetrie und Fernerkundung*, Springer-Verlag GmbH, Hannover, Deutschland, 65–103.

Kraus, K., 2004. *Photogrammetrie. Geometrische Information aus Photographien und Laserscanaufnahmen*. 7 edn, Walter de Gruyter GmbH Co. KG., chapter 1, 5.2., 3.4, 8.1.2.2.

Maas, H.-G., 2014. Geometrische Modelle der Mehrmedienphotogrammetrie. *Sonderheft avn (121) - Zeitschrift für Geodäsie und Geoinformation*. <https://gispoint.de/artikelarchiv/avn/2014/avn-ausgabe-32014/2534-geometrische-modelle-der-mehrmedienphotogrammetrie.html>.

Mandlbürger, G., 2019a. Through-Water Dense Image Matching for Shallow Water Bathymetry. *Photogrammetric Engineering Remote Sensing*, 85, 445-454.

Mandlbürger, G., 2019b. Through-Water Dense Image Matching for Shallow Water Bathymetry. *Photogrammetric Engineering Remote Sensing*, 85/6, 445-455.

Mandlbürger, G., 2020. A review of airborne laser bathymetry for mapping of inland and coastal waters. *Int. Arch. Photogramm. Remote Sens. Spatial Inf. Sci.*, XLIII-B1, 57–64.

Mandlbürger, G., Hauer, C., Wieser, M., Pfeifer, N., 2015. Topo-Bathymetric LiDAR for Monitoring River Morphodynamics and Instream Habitats—A Case Study at the Pielach River. *Remote Sensing*, 7, 6160-6195.

Mandlbürger, G., Otepka, J., Karel, W., Wagner, W., Pfeifer, N., 2009. Orientation and Processing of Airborne Laser Scanning Data (OPALS) - Concept and First Results of a Comprehensive ALS Software. *ISPRS Journal of Photogrammetry and Remote Sensing*, XXXVIII(Part 3/W8), 55-60.

Mandlbürger, G., Pfennigbauer, M., Pfeifer, N., 2013. Analyzing near water surface penetration in Laser Bathymetry - A case study at the river Pielach. *ISPRS Workshop Laser Scanning 2013*, 2, 175–180.

Mandlbürger, G., Pfennigbauer, M., Steinbacher, F., Pfeifer, N., 2011. Airborne hydrographic lidar mapping - potential of a new technique for capturing shallow water bodies. F. Chan, D. Marinova, R. Anderssen (eds), *MODSIM2011, 19th International Congress on Modelling and Simulation*, Modelling and Simulation Society of Australia and New Zealand, 2416–2422.

Mandlbürger, G., Rhomberg-Kauert, J., Gueguen, L.-A., Mulsow, C., Brezovsky, M., Dammert, L., Haines, J., Himmelsbach, T., Schulte, F., Amon, P., Winiwarter, L., Jutzi, B., Maas, H.-G., 2025. Mapping shallow inland running waters with UAV-borne photo and laser bathymetry. The Pielach River showcase. *Hydrographische Nachrichten*.

McCarthy, J., 2014. Multi-image photogrammetry as a practical tool for cultural heritage survey and community engagement. *Journal of Archaeological Science*, 43, 175–185.

Mildenhall, B., Srinivasan, P. P., Tancik, M., Barron, J. T., Ramamoorthi, R., Ng, R., 2020. NeRF: Representing Scenes as Neural Radiance Fields for View Synthesis.

Mulsow, C., 2010. A flexible Multi-media bundle approach. *The International Archives of the Photogrammetry*.

Mulsow, C., Mandlbürger, G., Maas, H.-G., 2020. Comparison of subaquatic digital elevation models from airborne laser scanning and imagery. *ISPRS Annals of the Photogrammetry, Remote Sensing and Spatial Information Sciences*, V-2-2020, 671–677. <https://isprs-annals.copernicus.org/articles/V-2-2020/671/2020/>.

Opitz, R., Cowley, D., 2013. Interpreting archaeological topography: Lasers, 3D data, observation, visualisation and applications. *Interpreting Archaeological Topography, Occasional publication of the Aerial Archaeology Research Group*, 5, 1-13.

Pfeifer, N., Mandlbürger, G., 2018. Lidar data filtering and digital terrain model generation. J. Shan, C. Toth (eds), *Topographic Laser Ranging and Scanning - Principles and Processing*, second edn, CRC Press, Boca Raton, 349–378.

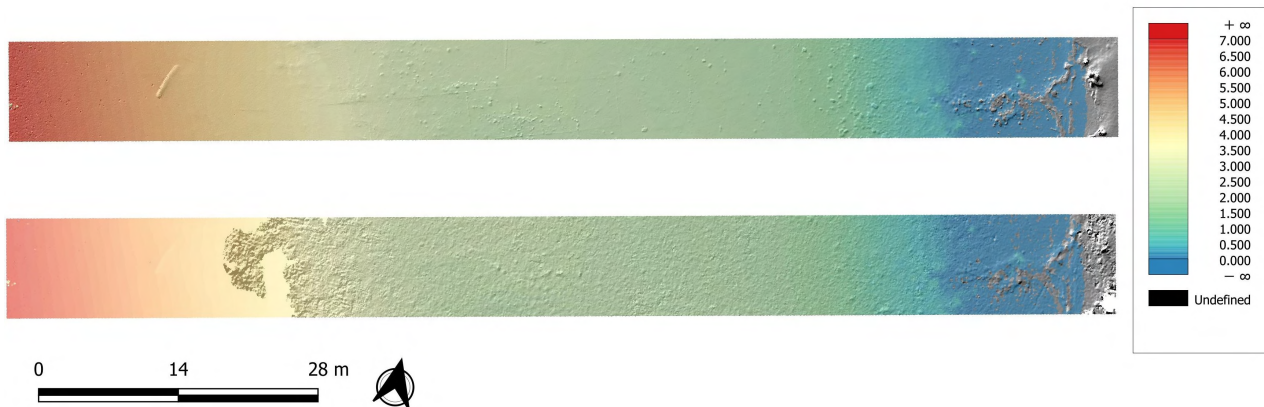


Figure 7. Results of the water depth model based on the bathymetric data. Top: DTM from the ALB and the water depth map; Bottom: DTM from Photobathymetry with the software Pix4D.

Pfeifer, N., Mandlbürger, G., Glira, P., 2017. Laserscanning. C. Heipke (ed.), *Photogrammetrie und Fernerkundung*, Springer-Verlag GmbH, Hannover, Deutschland, 431–481.

Pfeifer, N., Mandlbürger, G., Otepka, J., Karel, W., 2014. OPALS - A Framework for Airborne Laser Scanning Data Analysis. *Computers, Environment and Urban Systems*, 45, 125-136.

Philpot, W., Guenther, G., Lilycrop, J., Wozencraft, J., LaRocque, P., Penley, M., Pfennigbauer, M., Pe'eri, S., Feygels, V., Tingaker, T., Kopilevich, Y., Kim, M., Wang, C.-K., Parrish, C., Johnson, N., Macon, C., White, S., Eisemann, E., Reif, M., Dunkin, L., 2019. *BBII Airborne Laser Hydrography*. Cornell eCommons.

Pohl, H., 2015. *Bericht Zur Unterwasserarchäologischen Prospektion Station See/ Mondsee. 21.10.-31.12.2014" Fundberichte aus Österreich. 54, Österreichisches Bundesdenkmalamt, 2878–2897.*

Pohl, H., 2016. Drei Jahre unterwasserarchäologisches Monitoring an den österreichischen UNESCO-Welterbestätten „Prähistorische Pfahlbauten um die Alpen“. *Archäologie Österreichs*, 27(1), 29–35.

Pohl, H., 2018. Bericht Zur Unterwasserarchäologischen Prospektion Station See/ Mondsee. MNR 01.05.–31.12.2018 Fundberichte aus Österreich. *Fundberichte Österreichs 2018*, 57, 1-15. <https://www.academia.edu/49031814>.

Pohl, H., 2020. Bericht Zur Unterwasserarchäologischen Prospektion Station See/ Mondsee. MNR 05.10.–31.12.2020 Fundberichte aus Österreich. *Fundberichte Österreichs 2020*, 59, 1-10. <https://www.academia.edu/47410221>.

Pohl, H., 2021. Bericht Zur Unterwasserarchäologischen Prospektion Station See/ Mondsee. MNR 26.04.–03.05.2021 Fundberichte aus Österreich. *Fundberichte Österreichs 2021*, 60, 1-11. <https://www.academia.edu/83605265>.

Pohl, H., 2023. Monitoring See am Mondsee. *Prähistorische Pfahlbauten (online)*. <https://www.pfahlbauten.at/projekte/monitoring-see-am-mondsee>.

Pohl, H., Seidl da Fonseca, H., Dworsky, C., 2023. Kuratorium Pfahlbauten Monitoringbericht. Annual

report curatorship pile dwellings Austria. 1-38. <https://www.academia.edu/128958423>.

Rhomberg-Kauert, J., Dammert, L., Pfennigbauer, M., Mandlbürger, G., 2024. Macrophyte detection with bathymetric LiDAR - Applications of high-dimensional data analysis for submerged ecosystems. *International Hydrographic Review*, 30-2.

RIEGL, 2025. Website of VQ-840-G Topo-Bathymetric Airborne Laser Scanner. <http://www.riegl.com/nc/products/airborne-scanning/produktdetail/product/scanner/63/>. (10 June 2025).